Journal of Food Engineering 206 (2017) 23–36

Contents lists available at ScienceDirect

Journal of Food Engineering

journal homepage: www.elsevier.com/locate/jfoodeng

A novel method to improve heating uniformity in mid-high moisture potato starch with radio frequency assisted treatment

Hankun Zhu [a], Dong Li [a], Shujun Li [a, b, *], Shaojin Wang [c, d, **]

[a] College of Engineering, China Agricultural University, Beijing, 100083, China
[b] Chinese Academy of Agricultural Mechanization Sciences, Beijing, 100083, China
[c] College of Mechanical and Electronic Engineering, Northwest A&F University, Yangling, Shaanxi, 712100, China
[d] Washington State University, Department of Biological Systems Engineering, Pullman, WA, 99164-6120, USA

ARTICLE INFO

Article history:
Received 18 August 2016
Received in revised form
18 December 2016
Accepted 1 March 2017
Available online 2 March 2017

Keywords:
Mid-high moisture food
Uniformity
Electromagnetic distribution
RF
Potato starch
Simulation

ABSTRACT

An alternative method to improve treatment efficiency for industrial applications of mid-high moisture potato starch was explored based on radio frequency (RF) heating, but the large cold spot area during RF treatment was the biggest obstacle for technology development. The purpose of this study was to develop a new method to reduce the cold spot area and improve RF heating uniformity for mid-high moisture potato starch by modifying the electromagnetic field distribution in the sample with a Electromagnetic Wave Conductor (EWC). The simulation model of RF heating was established to study the temperature distribution using commercial COMSOL software. Dielectric properties of potato starch with moisture content of 31.55% w.b. were measured for computer simulation, and the associated RF experiments were conducted as the validation of the EWC method. The results showed that the parameters of EWC (width and height) had a positive correlation with the RF heating uniformity. The improved target uniformity index (TUI) and the decreased heating time indicated significant effects of EWC. Finally, optimizing EWC parameter equations were developed and could be used for improving RF heating uniformity in future applications.

1. Introduction

Mid-high moisture content (20%–50% wet basis) food materials are a large category, basically including raw, fresh, mashed and semi-finished foodstuff. Native starch is a good texture stabilizer and regulator in food systems and could be used for preparing different products (Ruan et al., 2009). Potato ranks fourth after wheat, rice and corn in production worldwide and a new potato staple food development plan has just been announced by Ministry of Agriculture in China (Lu, 2015). Industrial processing of potato starch includes washing, rasping, screening, filtering and drying. The starch with moisture content of about 30–40% w.b. after filtering needs to be dried to around 17% w.b. for safe storage in the drying process, which is commonly completed by hot air dryer (Talburt and Smith, 1987). In potato processing, traditional drying methods (hot air and drum dryer) with high temperatures result in high energy consumption, low heating efficiency and high production costs (Aviara et al., 2014; Gowda et al., 1991) with negative effects on the functions of starch (Bo and Tunde, 2013). Therefore, it is important to explore an alternative advanced drying or processing method to achieve high efficiency and product quality with low cost.

Electromagnetic energy has been proposed as a new alternative treatment method for agricultural product processing due to its fast and volumetric heating (Jiao et al., 2014; Wang and Tang, 2001). Radio frequency (RF) energy is a kind of electromagnetic wave for frequencies between 1 and 300 MHz, and has been widely used in baking (Koral, 2004), drying (Wang et al., 2011), pasteurization (Liu et al., 2011) and disinfestations (Wang et al., 2010) with high penetration depth and easy temperature control as compared to microwave heating (Wang et al., 2011). The major problem of RF treatments is the poor heating uniformity, especially for the

* Corresponding author. College of Engineering, China Agricultural University, Beijing, 100083, China.
** Corresponding author. College of Mechanical and Electronic Engineering, Northwest A&F University, Yangling, Shaanxi, 712100, China.
E-mail addresses: lisj@caams.org.cn (S. Li), shaojinwang@nwsuaf.edu.cn (S. Wang).

http://dx.doi.org/10.1016/j.jfoodeng.2017.03.001
0260-8774/

samples with higher moisture content (Huang et al., 2016).

Many studies have been carried out to improve the RF heating uniformity. For example, Birla et al. (2004) developed a fruit mover with pumped water to improve the RF heating uniformity of fresh fruit. Jiao et al. (2015) found that the similar dielectric constant surrounding material (polyetherimide, PEI) of the sample container is effective for the RF heating uniformity improvement in peanut butter. Huang et al. (2016) used polystyrene as a container material for dry soybeans to improve heating uniformity and studied the influence of container thickness on temperature distributions using computer simulation models. However, these methods are limited to dry food materials. It's desirable to study some new and practical methods for improving RF heating uniformity in potato starch with mid-high moisture content.

Based on the RF electromagnetic field distribution and bending characteristics (Birla et al., 2004), the problem of RF heating uniformity is mainly caused by the non-uniform electromagnetic distribution in the material and surrounding space, especially for the dielectric materials with higher moisture content (Birla et al., 2008; Farag et al., 2010; Tiwari et al., 2011). To improve the RF heating uniformity over the whole volume, the areas with less electromagnetic intensity need to introduce more energy by a conductor. Based on the electric force line bending theory between medias with different dielectric properties (TEC, 1987), the so-called electromagnetic wave conductor (EWC) with lower dielectric loss factor is introduced and placed inside the food sample to check if the RF heating uniformity could be improved.

The objectives of this study were 1) to measure the dielectric properties of potato starch with mid-high moisture content for computer simulation, 2) to establish RF heating simulation model of the sample with EWC, 3) to evaluate the heating uniformity and rate as influenced by EWC with different size, and 4) to optimize the EWC parameters (height and width) for achieving a uniform and efficient RF processing.

2. Materials and methods

2.1. Sample preparation

Standard refined potato starch (Maoyuan Inc., Pingliang, Gansu, China) was used in this study with the initial moisture content of 14.4% w.b. determined by standard oven method (SAC, 1985). In most of the potato starch industry, the moisture level of original materials in drying and modified starch processing is around 20%–40% (Sajilata et al., 2006; Zavareze et al., 2010). In this study, the moisture content of starch sample was adjusted to around 30% w.b. by adding predetermined quantity of distilled water. The preconditioned samples were gently mixed and shaken manually for 15 min. The samples were sealed in an isolated air-tight plastic bag at 4 °C for 4 d in a refrigerator to balance the moisture, and the bags were shaken 3 times per day during storage. The sample bags were taken out from the refrigerator after equilibrium and put in an incubator (BSC-150, Shanghai BoXun Industrial & Commerce Co., LTD., Shanghai, China) at 23 °C for one more day to obtain uniform initial sample temperature before the experiment (Huang et al., 2016; Wang et al., 2015b). The final moisture content of the adjusted starch was 31.55% w.b. for dielectric properties measurement and RF treatments.

2.2. Dielectric properties measurement with physical properties

The open-ended coaxial probe technique is a popular method for measuring dielectric properties and usually used for liquid or semi-solid materials over a broad frequency range. In this study, potato starch was compressed into cylindrical samples by a stainless steel cylindrical holder (diameter 21 mm and height 85 mm) and contacted tightly with the probe (Guo et al., 2010; Ling et al., 2014; Zhang et al., 2016). Dielectric properties measurement system consisted of an Agilent 85070E open-ended coaxial probe, an Agilent E4991B vector impedance analyzer (Agilent technologies, California, U.S.A.), and a computer with 85070E dielectric probe kit software (Agilent technologies, California, U.S.A.). The sample was confined in the cylindrical holder with a spring to ensure a close contact between the tip of the coaxial probe and the sample during the measurements. The sample temperature was controlled by circulating oil from an oil bath (LNEYA SST-20, Wuxi Guanya Constant Temperature Cooling Technology Co., Ltd., Wuxi, China) into the jacket of the test holder. The sample center temperature during measurement was monitored by a thermocouple (HH-25TC, Type-T, OMEGA Engineering Inc., Stamford, Connecticut, USA) to reach 4 selected measuring temperatures (30, 40, 50, and 60 °C), which were based on the safe temperature to protect starch quality (Çatal and İbanoğlu, 2012). Measurements of starch dielectric properties were conducted in two replicates at each selected temperature. Before the measurement, the analyzer was turned on for about 30 min for warming up and then calibrated with open, short and 50 Ω load in sequence. The open-ended coaxial probe and coaxial-cable were then attached to the system, and further calibrated with air, short probe, and 25 °C distilled water.

Bulk density of potato starch with moisture content of 31.55% w.b. at room temperature was measured by a basic volume method with a 132 × 184 × 64 mm^3 polypropylene rectangular container and determined to be 770 ± 2 kg m^{-3} based on three replicate measurements. Thermal conductivity and heat capacity of potato starch sample were 0.3247 W $m^{-1}k^{-1}$ and 2350 J kg^{-1} K^{-1} at the 45 °C based on the study of Ryynänen (1995) and Noel and Ring (1992), respectively. Table 1 lists physical properties of the container, and surrounding materials, including polystyrene (EWC), polypropylene (container), aluminum (RF system), and air, for computer simulation.

2.3. Determination of EWC

In RF heating for bulk materials, non-uniform electromagnetic

Table 1
Electrical and physical properties of polystyrene, polypropylene, air, and aluminum used in simulation modelling.

Container and surrounding material	Density (kg m^{-3})	Thermal conductivity (W m^{-1} K^{-1})	Heat capacity (J kg^{-1} K^{-1})	Dielectric constant (ε')	Loss factor (ε'')
Polystyrene	25[a]	0.036[a]	1300[a]	2.6[b]	0.0003[b]
Polypropylene[c]	900	0.26	1800	2.0	0.0023
Air[d]	1.2	0.025	1200	1	0
Aluminum[d]	2700	160	900	1	0

[a] Juran (1991).
[b] Brandrup et al. (1989).
[c] Von Hippel (1954).
[d] COMSOL material library (2012).

energy distribution results in cold spots at the central area and overheating at the corner or edge portion of the sample (Tiwari et al., 2011), especially for the materials with higher moisture content (Huang et al., 2016). To further improve the volumetric heating uniformity of RF treatments for bulk materials with higher moisture content, EWC was introduced. Polystyrene was selected as the material of EWC for its low loss factor, thermal conductivity and water absorption (Juran, 1991), which may provide small electromagnetic wave transferring impedance and low thermal conductivity. To introduce more electromagnetic wave into the central area of the sample, the EWC was designed to crossed cuboids based on high throughput and efficiency, and the introduced electromagnetic field direction in the rectangular container. This cross shaped EWC might improve the central cold spot area coordinately in three vertical directions with multiple contacting areas, and also take less space in the container. Each end of the EWC sheet was contacted with the walls of container to avoid overheating (Fig. 1).

2.4. Computer simulation

2.4.1. Geometrical model of RF heating

The RF system included a generator and heating cavity. RF energy was generated by an oscillation circuit in the generator and matched into heating cavity through a feeding strip. High intensity electromagnetic field was formed between two parallel aluminum plate electrodes, and the adjustable electrode gap determines different output power in dielectric materials. The potato starch sample with EWC was put in the center of bottom electrode (Fig. 2). Dimensions of the RF cavity and the attached parts in simulation model can be found in former study (Chen et al., 2016; Huang et al., 2015). Based on preliminary experiments, the electrode gap was set at 110 mm to heat the starch sample at a reasonable heating rate.

2.4.2. Governing equations

RF simulation was based on the simultaneous solution of heat transfer coupled with electromagnetic field displacement in the multi-domains (samples and the surrounding environment) inside the RF cavity. Electromagnetic field distribution inside the RF applicator was described by four Maxwell's equations of electromagnetism in differential forms, which could be expressed in terms of the electric field (E) and magnetic intensity (H) as follows (Balanis, 1989):

$$\nabla \cdot \vec{D} = \rho_e \tag{1}$$

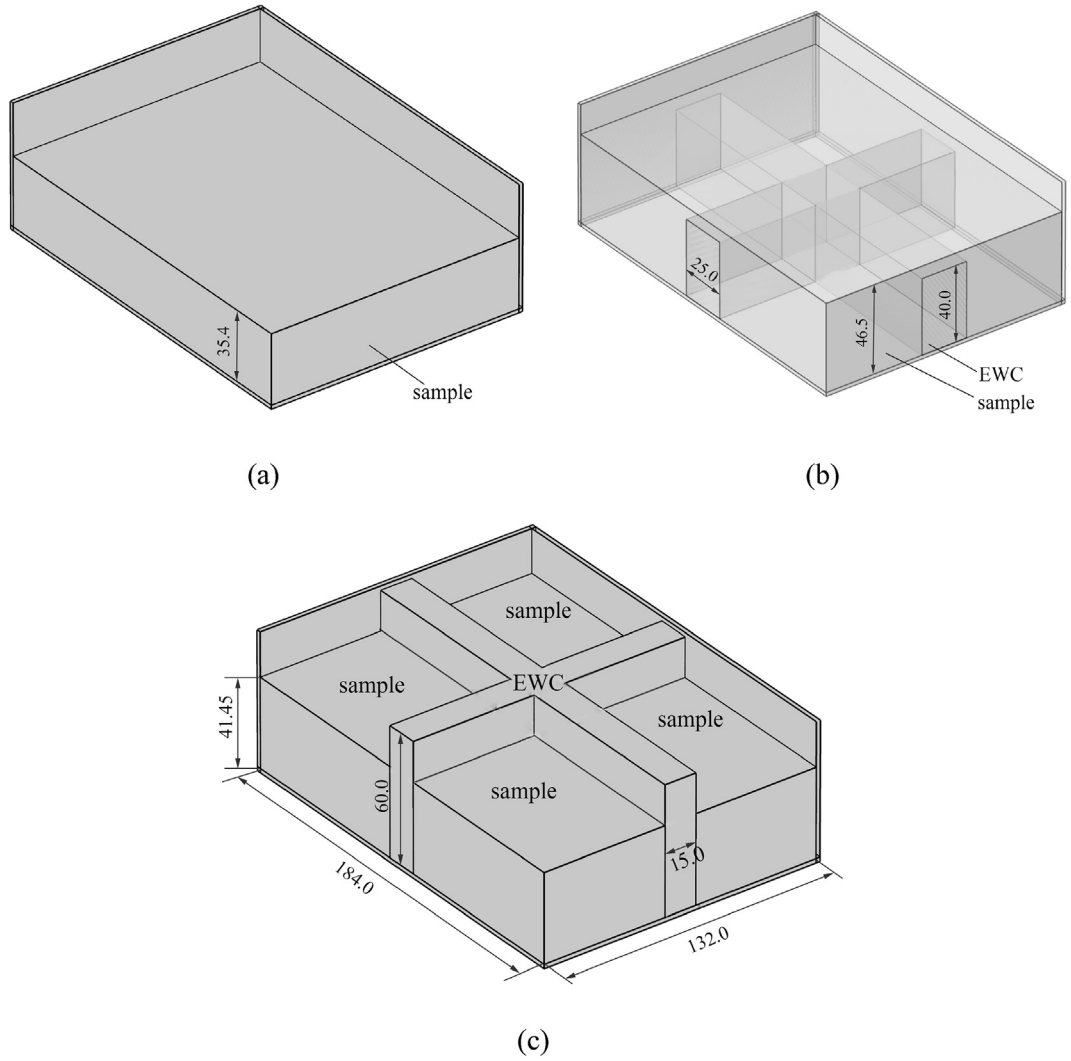

Fig. 1. Sketches of the sample in the container without (a) and with EWC sheets at lower height (40 mm height and 25 mm width) (b), and higher height (60 mm height and 15 mm width) (c). All the dimensions are in mm.

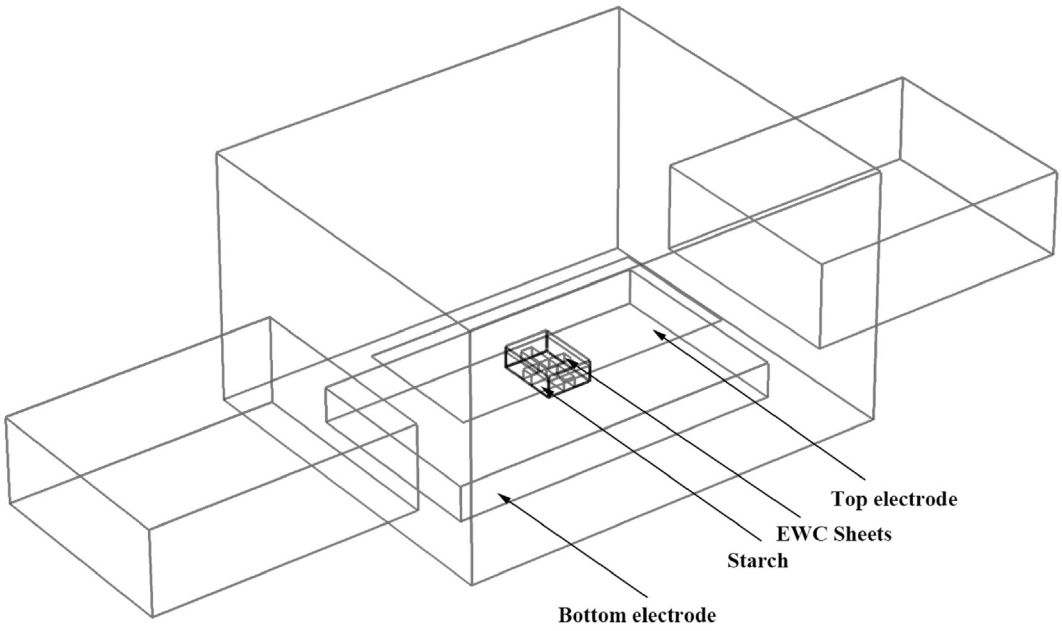

Fig. 2. Simulation model of the sample with EWC sheets in the RF cavity.

$$\nabla \cdot \vec{B} = 0 \tag{2}$$

$$\nabla \cdot \vec{E} = \frac{\partial \vec{B}}{\partial t} = -\mu \frac{\partial \vec{H}}{\partial t} \tag{3}$$

$$\nabla \cdot \vec{H} = \vec{J} + \frac{\partial \vec{D}}{\partial t} = \varepsilon \frac{\partial \vec{E}}{\partial t} + \varepsilon_0 \varepsilon'' \omega \vec{E} \tag{4}$$

where D is the electric flux density (C m^{-2}), B is the magnetic flux density (Wb m^{-2}), ρ_e is the total electric charge density (C m^{-3}), E is the electric field intensity (V m^{-1}), H is the magnetic field intensity (A m^{-1}), μ is the magnetic permeability (H m^{-1}), J is the total current density (A m^{-2}), ω is the angular frequency (rad s^{-1}), and ε is the complex relative permittivity of the dielectric material (F m^{-1}), which can be expressed in terms of the relative (to air) dielectric constant (ε') and the relative loss factor (ε'') of the material ($\varepsilon = \varepsilon' - j\varepsilon''$).

The absorbed RF power density at any point inside the material is proportional to the square of the electric field strength, the dielectric loss factor and the frequency as follows (Choi and Konrad, 1991):

$$Q = 2\pi f \varepsilon_0 \varepsilon'' E_r^2 = \pi f \varepsilon_0 \varepsilon'' \left|\vec{E}\right|^2 \tag{5}$$

where Q is the power conversion to thermal energy in foods (W m^{-3}), f is the frequency (Hz), ε_0 is the permittivity of electromagnetic wave in free space (8.86×10^{-12} F m^{-1}), ε'' is the loss factor of food material, E_r is the root mean square value of the electric field (V m^{-1}), and the scalar voltage potential (V) is related to the electric field as $\vec{E} = -\vec{\nabla} V$.

Heat convection at the material's surface and the heat conduction within the sample (starch), is described by the equation (Nelson, 1996):

$$\rho C_p \frac{\partial T}{\partial t} = \vec{\nabla} \cdot k \vec{\nabla} T + Q \tag{6}$$

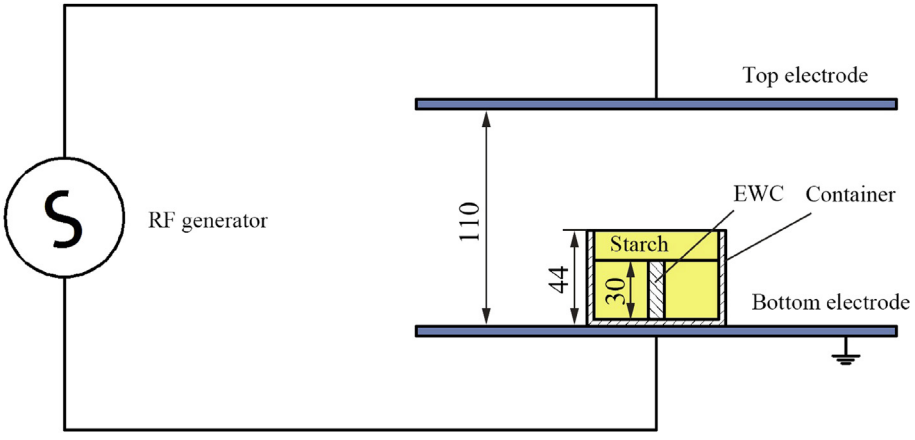

Fig. 3. Schematic of RF heating for potato starch at moisture content of 31.55% with EWC.

where $\partial T/\partial t$ is the heating rate in food material (°C s^{-1}), α is the thermal diffusivity (m^2 s^{-1}), ρ and C_p are the density (kg m^{-3}) and heat capacity (J kg^{-1} K^{-1}), respectively.

Convective heat transfer was considered on the external surfaces of starch, which can be described as (Huang et al., 2015):

$$-k\vec{\nabla}T\vec{n} = h(T - T_{air}) \quad (7)$$

where h is convective heat transfer coefficient ($h = 20$ W m^{-2} K^{-1} for natural convection), T_{air} is the air temperature ($\approx$23 °C) and $\vec{n}$ is the vector of the surface crossed by the heat flux.

2.4.3. Initial and boundary conditions

The metal enclosure boundary of RF unit was considered as thermal insulation ($\nabla T = 0$). The top electrode was set as the electromagnetic source since it introduced the high frequency electromagnetic energy from the generator to the heating cavity and the bottom electrode was set as ground ($V = 0$ V). Electrical insulation $\vec{\nabla} \cdot \vec{E} = 0$ was considered for the external walls of the RF cavity. The surrounding air was considered in the inlet and outlet of the system with condition of $T = T_{air}$. The initial temperature of all domains in the system, including the air, plastic container, starch, upper and bottom electrodes was set at 23 °C.

Voltage of the top electrode can be determined by anode current (I_a) with the linear equation (Zhu et al., 2014):

$$V = 10401 \times I_a + 1974.1 \quad (8)$$

A constant electric field strength was assumed and applied at the upper electrode during the processing time, because 30% of the RF wavelength (11 m) is larger than the dimension of the upper electrode (830 × 400 mm^2) in the operating RF system and voltage variation is less than 10% (Wang et al., 2015a).

2.4.4. Solving and meshing procedure

A DELL workstation with Core i7 processors, 12 GB RAM on a Windows 7 64 bit operating system was used to run the finite element software COMSOL (V4.3a, COMSOL Multiphysics, Burlington, MA, USA) for solving the RF multi-physics heating model and evaluate the heating pattern of the sample with EWC. Fine tetrahedral mesh was generated in the sample, EWC and the top electrode to guarantee the accuracy of temperature distribution results. The maximum and minimum element sizes were 231 and 28.9 mm, respectively, and the number of the elements in the model was 25,883 for the sample with EWC of 50 mm height and 35 mm width. Other parts of the model were meshed with normal size tetrahedral meshes. Mesh size was chosen based on the convergence study when the difference in the resulted temperatures between successive calculations was less than 0.1%. The initial and maximum time steps used in this study were set as 0.001 and 1 s.

2.5. RF heating experiment

RF heating experiment was conducted with a 6 kW free-running oscillator RF system (SO6B, Strayfield International, Wokingham, UK), and the running schematic was shown in Fig. 3. In experiment, different kinds of EWC sheets were respectively put inside the 500 g potato starch with moisture content of 31.55% w.b. at a rectangular polypropylene container (132 L × 184 W × 64 H mm^3). Each of the samples was divided into 2 layers based on the half of the weight by a gauze (with mesh opening of 0.7 mm) for easily mapping the surface sample temperature of each layer. The samples with EWC were put in the center of the bottom electrode with 110 mm electrode gap. To avoid potato starch partially gelatinization at the moisture concentrated part, the heating temperature of each experiment should not largely exceed the limited temperature (around 64 °C) of potato starch (Çatal and İbanoğlu, 2012). Thus, the target temperature of RF heating was set at 60 °C and 4 fiber optic sensors (FTS-P104, HeQi Opto-Electronic Technology, Xi' an, Shaanxi, China) with an accuracy of ±1 °C were used to monitor sample temperatures at 4 corner points in the middle layer. When one of the sensors reached 60 °C, the RF system was turned off. The container was immediately moved out for temperature mapping with an infrared thermal imaging camera (DM63, Dali Science and Technology, Hangzhou, Zhejiang, China) with an accuracy of ±2 °C. Each experiment was repeated two times.

2.6. EWC effect on RF heating uniformity

2.6.1. Heating uniformity evaluation

Effect of EWC sheets on the improvement of heating uniformity was compared and evaluated based on the uniformity index from simulation results. To better reflect the degree to which temperature in the volume deviated from the target temperature for higher moisture food material, the target uniformity index (TUI) developed by Jiao et al. (2015) was introduced in this study:

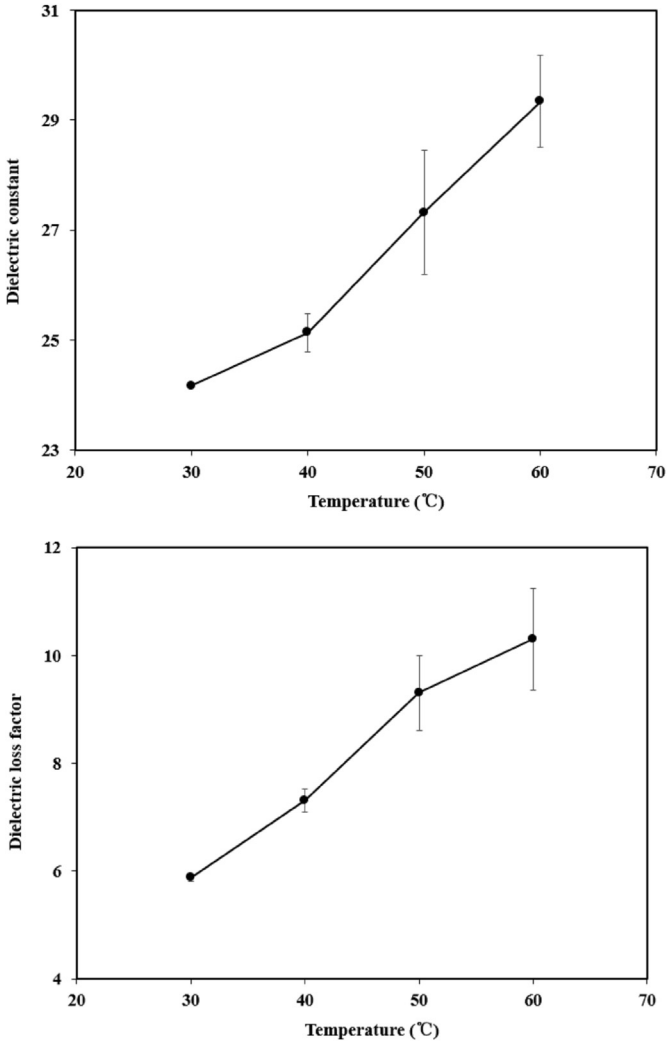

Fig. 4. Temperature-dependent dielectric constant (a) and loss factor of potato starch with moisture content of 31.55% w.b. at 27.12 MHz.

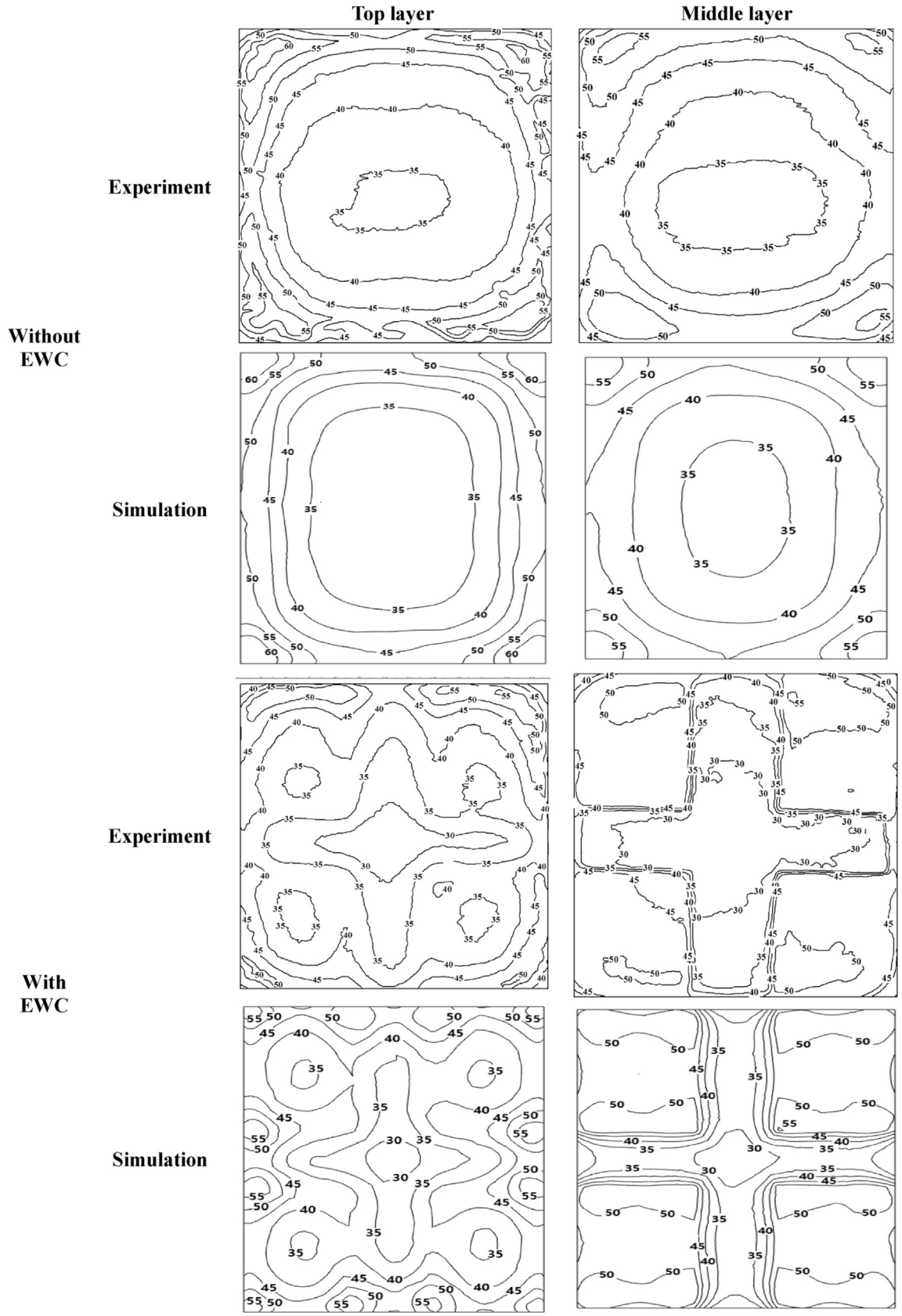

Fig. 5. Simulated and experimental temperature distributions (°C) of potato starch with moisture contents of 31.55% w.b. in top and middle layers placed in the polypropylene container on the center of bottom electrode after RF heating at the electrode gap of 110 mm and initial temperature of 23 °C without and with EWC sheets (50 mm height and 35 mm width).

$$TUI = \frac{\int_{V_{vol}} |T - T_t| dV_{vol}}{(T_t - T_{initial})V_{vol}} \quad (9)$$

where T_t is the target heating temperature (°C), $T_{initial}$ is the initial temperature of the sample (°C), and V_{vol} is the volume of food (m^3). Smaller uniformity index indicated better heating uniformity for the selected domain in simulation model.

2.6.2. Influence of EWC width and height on heating uniformity

The effect of EWC on RF heating uniformity in potato starch with mid-high moisture was determined by the EWC sizes (height and width). In this study, the heights of EWC sheets were swept from 20 mm to 60 mm with an interval of 10 mm for three selected EWC widths of 15, 25 and 35 mm, which were used both in the experiment and simulation to investigate the effect of EWC size on TUI and temperature distribution. To effectively obtain the better EWC parameters (width and height), a series of test methods and correlation equations were developed based on the size of both container and sample.

2.6.3. Effects of EWC on RF heating rate

RF heating rate may directly influence the tolerance of both microorganism's survival and food product quality. RF heating rate in samples was largely affected by the EWC size. RF heating time in potato starch samples with various EWC sizes was recorded to compare the heating rate.

3. Results and discussion

3.1. Dielectric properties of the sample

The mean values of temperature dependent dielectric properties of potato starch at 27.12 MHz and temperature range from 30 to 60 °C are shown in Fig. 4. The average dielectric constant increased from 24.16 to 29.34 and loss factor increased from 5.88 to 10.30 when the temperature increased from 30 to 60 °C. Similar trends have also been found in other starches (Ndife et al., 1998) and peanut flour (Zhang et al., 2016). The dielectric properties of potato starch were further used in the computer simulation model and inputted as linear interpolation functions with temperature in the simulation program.

3.2. Top electrode voltage estimation

Top electrode voltage of RF heating is an important input parameter for computer simulation, and can be estimated based on

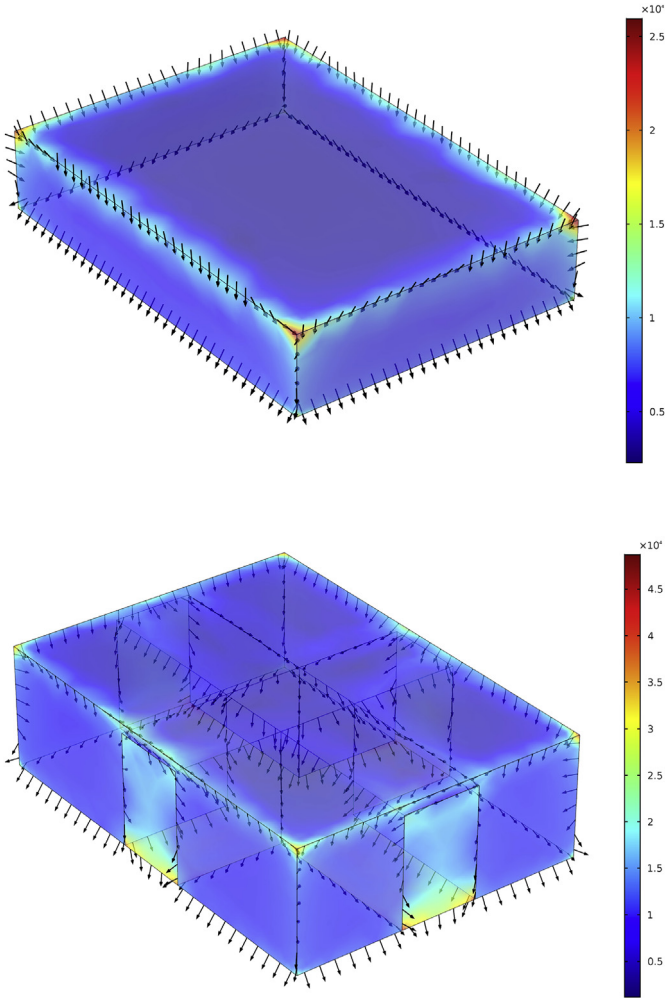

Fig. 6. Electric field intensity (V/m) and directions in the potato starch sample at terminated time with moisture content of 31.55% treated by RF energy at electrode gap of 110 mm without (a) and with (b) EWC sheets (50 mm height and 35 mm width).

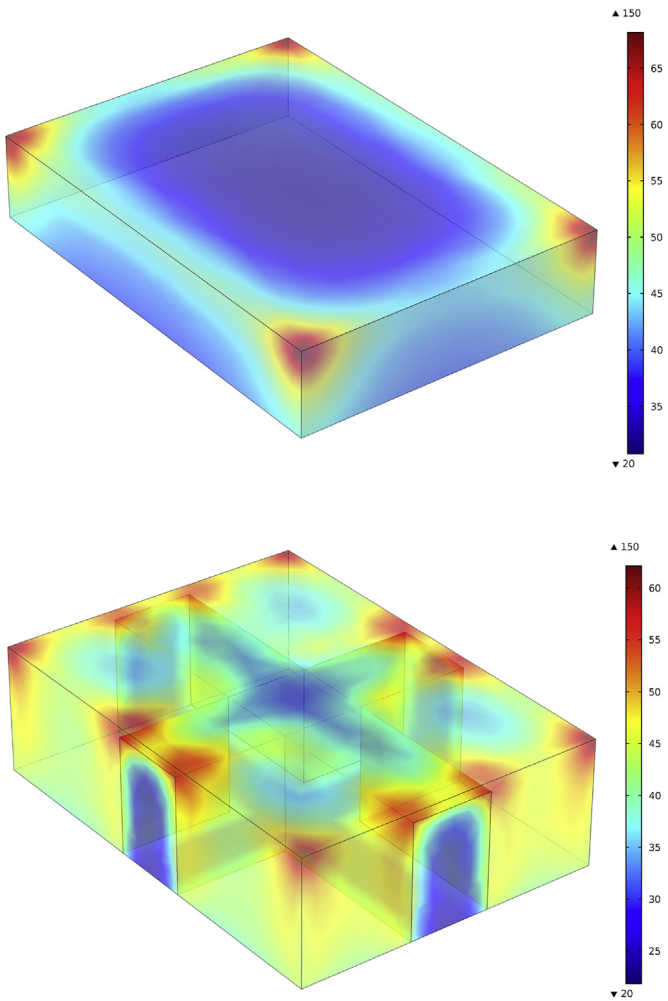

Fig. 7. Overall heating patterns (°C) of the potato starch sample treated by RF energy at electrode gap of 110 mm and initial temperature of 23 °C without (a) and with (b) EWC sheets (50 mm height and 35 mm width).

the study of Zhu et al. (2014) and Wang et al. (2015b). The anode current of RF heating in potato starch with different kinds of EWC sheets remained at 0.31 A, and its corresponding estimated top electrode voltage was around 5198.3 V. The small variation of anode current with EWC was probably caused by the small treatment scale of the starch sample, which was not enough to change the RF system output parameters obviously.

3.3. Simulation model validation

Fig. 5 shows the top and middle layer surface temperature contours of the starch sample (31.55% w.b.) with and without EWC sheets obtained from experimental and simulated results. Both simulated contours of starch sample with and without EWC were in good agreement with the experimental results. The maximum temperature difference in top and middle sample layers was 43.01 °C and 26.33 °C without EWC, respectively, and 33.83 °C and 11.65 °C for the sample with EWC (width 35 mm with height 50 mm). As Fig. 5 shows, the sample with EWC had better heating uniformity patterns than that without EWC sheets, especially in the middle layer, for the large cold spot area at central part of the sample without EWC was almost eliminated as the EWC introduced

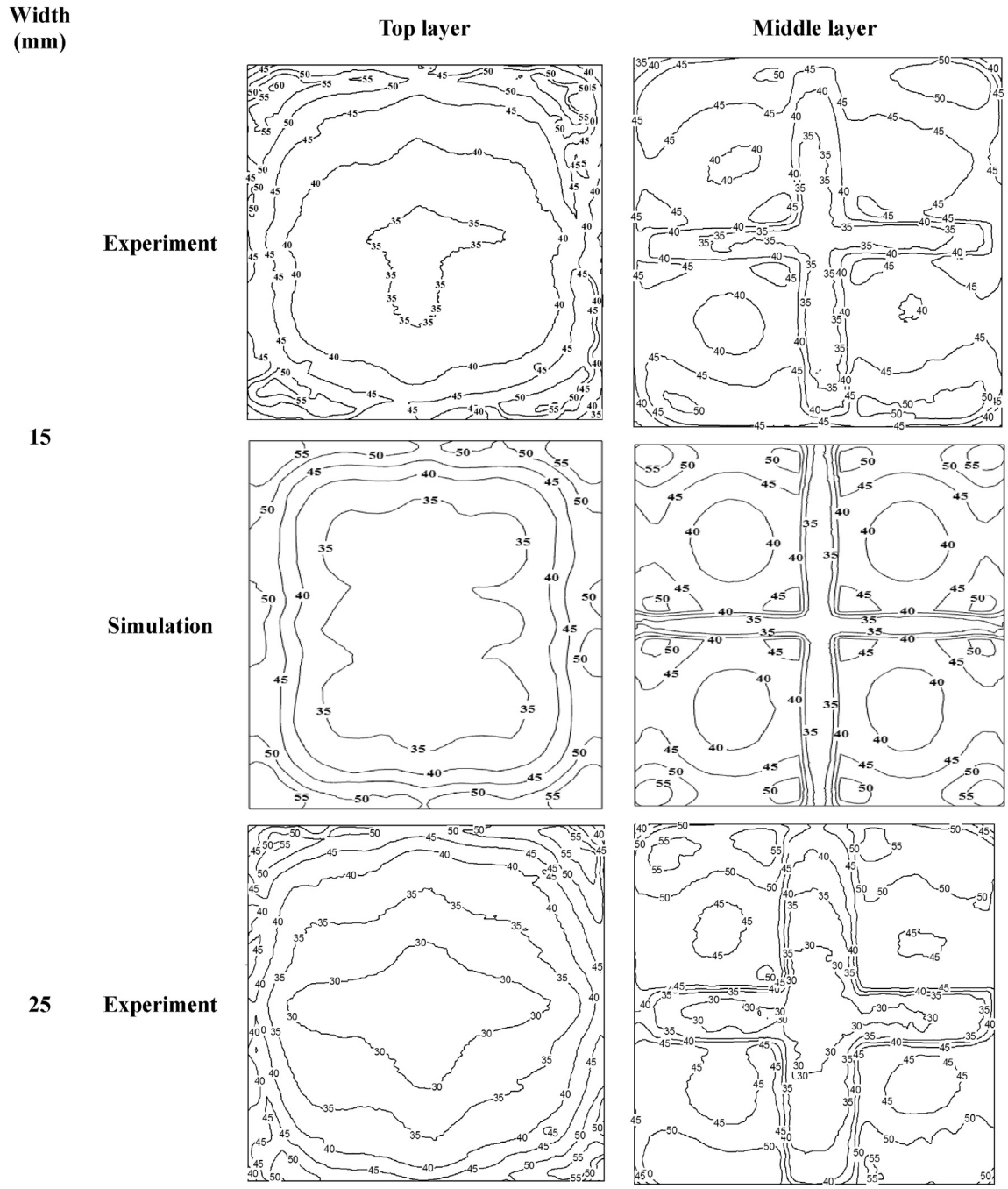

Fig. 8. Simulated and experimental temperature distributions (°C) of potato starch with moisture contents of 31.55% w.b. in top and middle layers placed in the polypropylene container on the center of bottom electrode after RF heating at the electrode gap of 110 mm and initial temperature of 23 °C with different EWC widths (15, 25, and 35 mm) and determined height of 30 mm.

more electromagnetic energy on it. The highest temperature spot was found in the top layer of simulated results, which may be caused by less thermal loss in the model than experimental results due to slightly longer temperature mapping.

3.4. Effect of EWC on heating patterns and uniformity

3.4.1. Effect of EWC on electric field distribution

The value and direction of electric field intensity in the starch samples with and without EWC sheets are shown in Fig. 6. The electric field distribution at cold spot area in the central part of the sample changed clearly and the electric field distribution seemed more uniform at each part of the sample as comparison between the models with and without EWC. The effect of EWC was caused by the function of EWC based on the electromagnetic bending theory (TEC, 1987) that introduced electromagnetic energy not only into central area of sample vertically, but also horizontally conducted through the contact area between the sample and EWC. As the simulation model indicated, EWC (height 50 mm and width 35 mm) raised volume average electric intensity from 4.17×10^3 to 7.29×10^3 Vm^{-1} as compared to the sample without EWC. The arrows in Fig. 6 indicated electric field directions, and electric field lines concentrated both at the edge of the sample and EWC sheet. Thus, the utilization of EWC sheets tremendously changed the electromagnetic distribution in the sample, and then improved the volumetric RF heating uniformity in the mid-high moisture food material.

3.4.2. Effect of EWC on overall heating patterns

Fig. 7 shows the overall temperature distributions of the potato

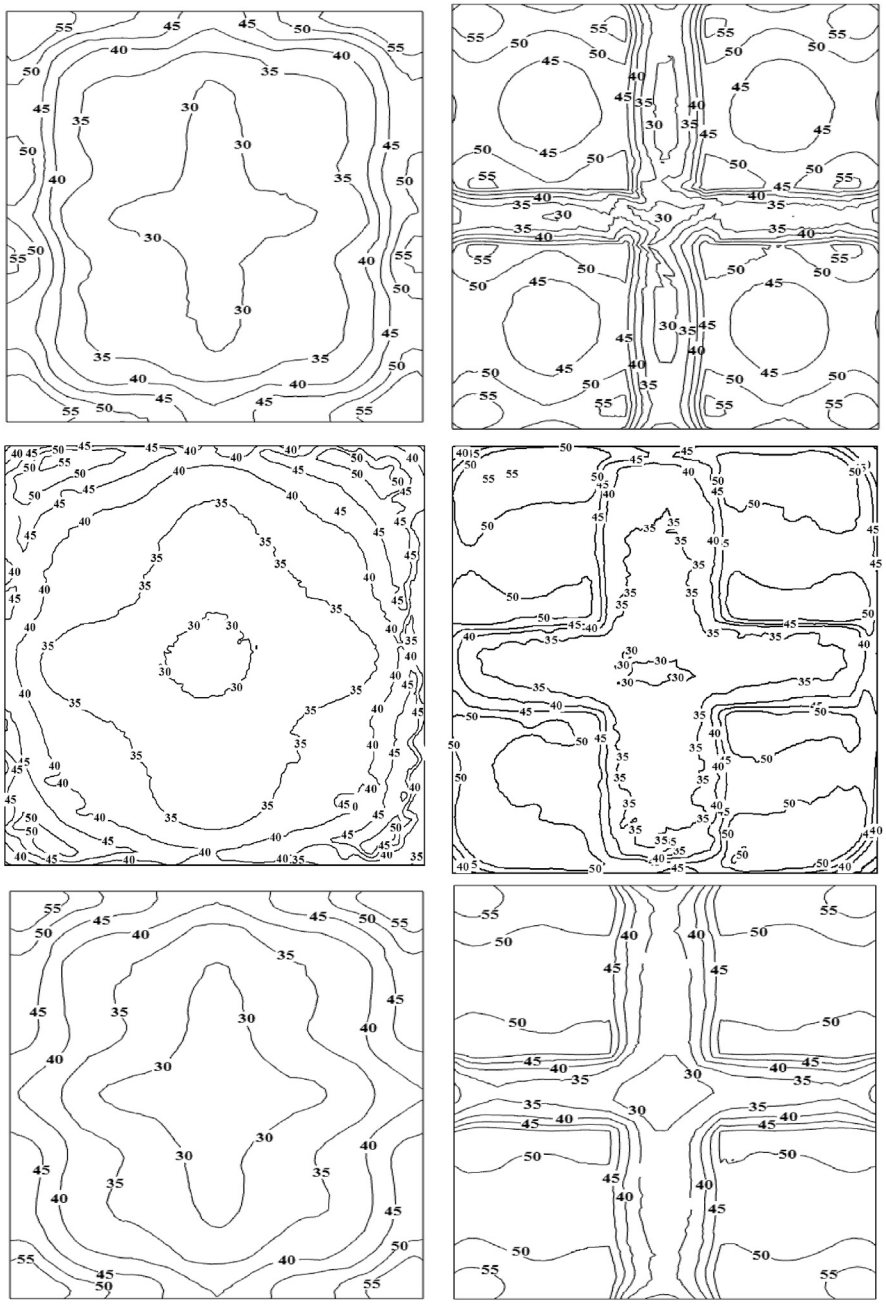

Fig. 8. (*continued*).

starch sample treated by RF energy at electrode gap of 110 mm without and with EWC sheets. For the sample heated without EWC sheets, the cold spot area was largely concentrated at the central area over the whole container (Fig. 7a). With adding EWC (width 35 mm with height 50 mm), the overall heating patterns was changed clearly and the thermal distribution of the sample seemed more uniform than that of the sample without EWC (Fig. 7b). The cold spot area at central part of the sample was divided into four minimized parts by EWC sheets during RF heating, resulting in improving the heating uniformity. The volume average temperature of the sample without EWC was 41.57 °C with heating time of 340 s, compared to that of 47.58 °C with EWC in the heating time of 178 s, thus, the dual inter-related functions of EWC on the sample with RF heating were both reflected on thermal distribution and heating rate. The calculated TUI for RF heating uniformity improvement method is listed in Table 4. For the sample without EWC, TUI was 0.460 as compared to that of 0.283 with EWC (width 35 mm with height 50 mm), which indicated that the heating uniformity of potato starch sample with moisture content of 31.55% was improved by EWC effectively.

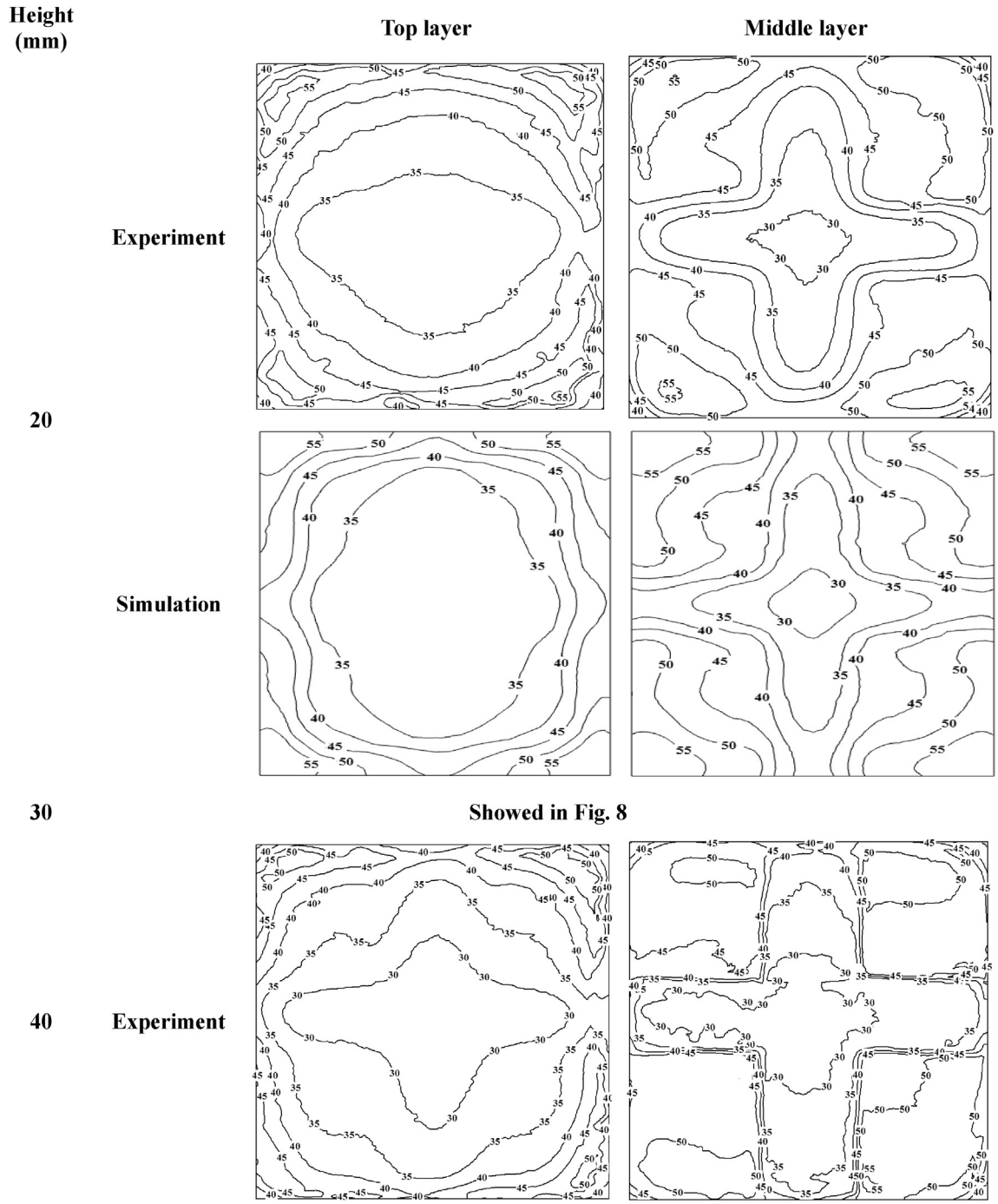

Fig. 9. Simulated and experimental temperature distributions (°C) of potato starch with moisture contents of 31.55% w.b. in top and middle layers placed in the polypropylene container on the center of bottom electrode after RF heating at the electrode gap of 110 mm and initial temperature of 23 °C with different EWC heights (20, 30, 40, 50, and 60 mm) and determined width of 35 mm.

3.4.3. Effect of the EWC width and height

Figs. 8 and 9 with Tables 2 and 3 show the experimental and simulated temperature contours and associated values of starch in top and middle layers with different EWC sizes. Table 4 shows the volume average temperature and TUI for the potato starch samples treated with and without EWC. As EWC width increasing, the average temperature of the middle layer increased from 45.69 to 50.95 °C with the standard deviation decreased from 4.88 to 3.14 °C (Table 2), and TUI decreased from 0.430 to 0.368, from 0.419 to 0.342 and from 0.420 to 0.293, respectively, for the corresponded EWC heights of 20, 30 and 40 mm (Table 4). The improvement of RF heating uniformity can also been seen directly in Fig. 8. Thus, the width of EWC had positive correlation with the heating uniformity. For increasing the EWC height, the average middle layer temperature increased from 43.71 to 50.44 °C associated with the standard deviation dropped from 9.62 to 2.30 °C (Table 3). As the EWC height increasing, TUI decreased from 0.430 to 0.420, from 0.396 to 0.349, and from 0.368 to 0.284, respectively, for 3 different EWC widths of 15, 25 and 35 mm (Table 4). Therefore, the RF heating uniformity can also be improved by adding the height of EWC sheets. However, as Table 4 indicated, when the height of EWC exceeded the 40, 50, and 60 mm for the EWC with widths of 15, 25 and 35 mm, respectively, the TUI indicated a slight rise from that of the previous value. This interesting phenomenon can also be observed in Fig. 9

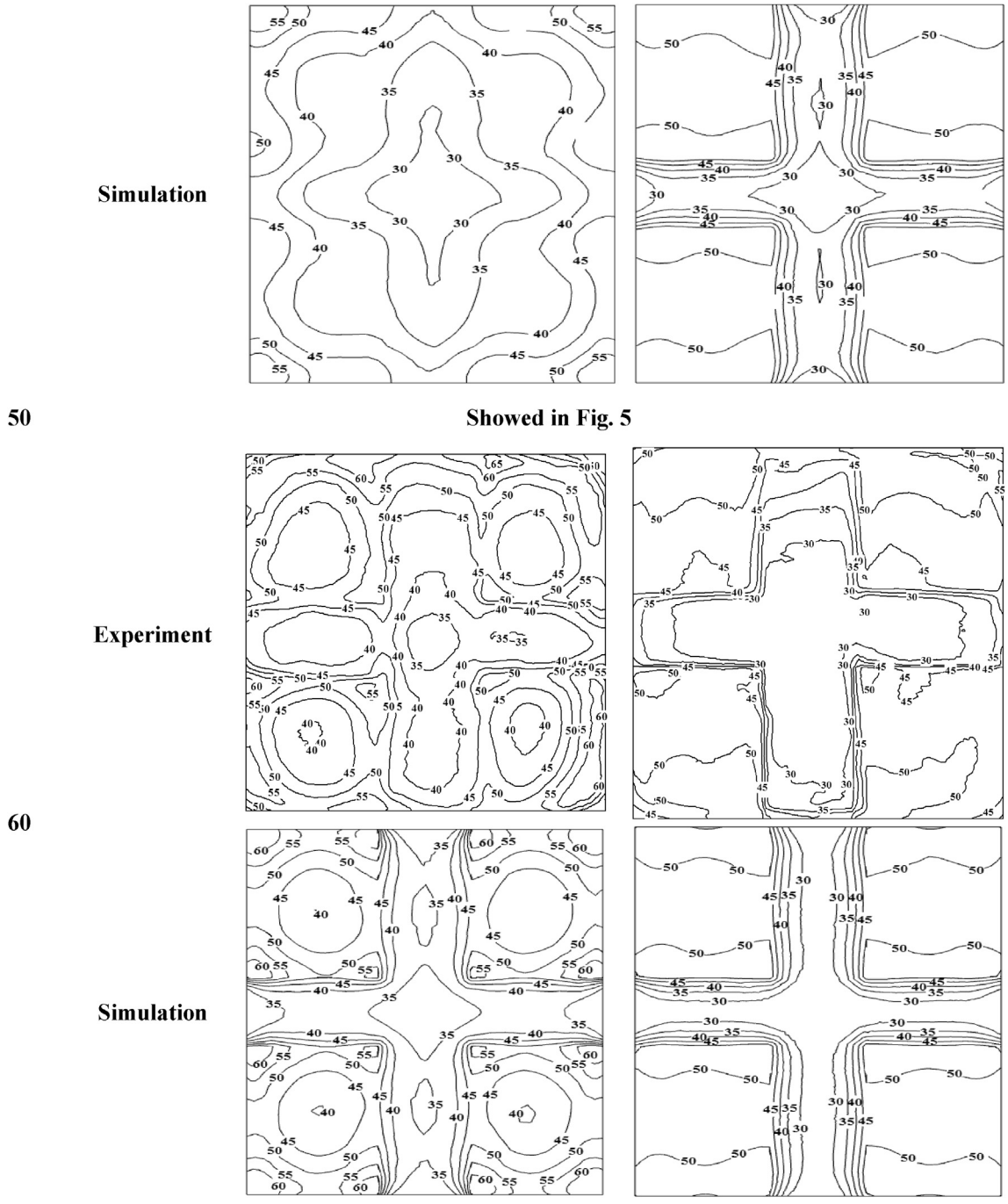

Fig. 9. (*continued*).

Table 2
Simulated minimum (Min), maximum (Max), average (Avg) and standard deviation (Std) temperatures (°C) of potato starch with moisture content of 31.55% w.b. in two horizontal layers (top and middle) with various EWC widths and determined height of 30 mm after RF heating with a fixed electrode gap of 110 mm and initial temperature of 23 °C.

EWC width (mm)	Layer	Min (°C)	Max (°C)	Avg (°C)	Std (°C)
Without	Top	30.36	81.47	46.89	12.23
	Mid	32.30	60.33	44.34	7.88
15	Top	29.78	78.08	44.80	10.22
	Mid	37.88	57.17	45.69	4.88
25	Top	28.15	78.38	45.38	11.14
	Mid	41.79	56.96	48.63	3.71
35	Top	26.93	74.91	43.67	11.22
	Mid	45.03	57.68	50.95	3.14

Table 3
Simulated minimum (Min), maximum (Max), average (Avg) and standard deviation (Std) temperatures (°C) of potato starch with moisture content of 31.55% w.b. in two horizontal layers (top and middle) with various EWC heights and determined width of 35 mm after RF heating with a fixed electrode gap of 110 mm and initial temperature of 23 °C.

EWC Height (mm)	Layer	Min (°C)	Max (°C)	Avg (°C)	Std (°C)
20	Top	28.33	77.73	44.52	11.82
	Mid	27.53	62.92	43.71	9.62
30	Top	26.93	74.91	43.67	11.22
	Mid	45.03	57.68	50.95	3.14
40	Top	27.13	66.20	44.25	8.98
	Mid	45.17	54.52	50.31	2.55
50	Top	27.77	61.60	44.92	7.28
	Mid	44.20	55.85	50.36	2.63
60	Top	37.50	70.99	51.01	7.78
	Mid	45.73	54.63	50.44	2.30

Table 4
Simulated volume average temperature (VAT, °C) and target uniformity index (TUI) of starch with moisture content of 31.55% w.b. with various EWC heights after RF heating with a fixed electrode gap of 110 mm.

EWC Height (mm)	Parameter	EWC width (mm)		
		15	25	35
Without	VAT	41.57		
	TUI	0.460		
20	VAT	42.89	44.14	44.89
	TUI	0.430	0.396	0.368
30	VAT	42.98	44.31	45.41
	TUI	0.419	0.382	0.342
40	VAT	43.20	45.37	45.89
	TUI	0.420	0.347	0.293
50	VAT	43.20	45.58	47.58
	TUI	0.420	0.349	0.283
60	VAT	43.20	45.58	47.36
	TUI	0.420	0.349	0.284

through the comparison between sample top layer contours with EWC heights of 50 mm and 60 mm. This may be caused by the influence of revealing EWC sheets intensified the electromagnetic field bending effect in the air space between the sample and top electrode as the function of dielectric properties difference of air, potato starch sample and EWC (TEC, 1987). Therefore, to effectively improve the volume heating uniformity, optimizing sizes of EWC is necessary.

3.5. Effect on heating rate

As Fig. 10 indicated, the heating time of starch sample to the target temperature varied due to influence of EWC size. Because the EWC size determines both the overall sample height affecting the matching effect of the sample to the system (Strayfield, 2012; Tiwari et al., 2011) and the contact area between the sample and EWC, RF heating time decreased with increasing EWC volume as the function of the EWC height or width. For the potato starch sample heated by RF systems without EWC in this study, the heating time was 340 s, compared to that of 167 s with EWC size of 60 mm height and 35 mm width. As results show, with increasing EWC height from 20 to 60 mm, the heating time for three different EWC widths (15, 25, and 35 mm) decreased to 72 s, 85 s and 100 s, respectively. The decreasing heating time of the sample as the function of EWC size indicated that the heating rate can be adjusted by adding different EWC size.

3.6. EWC parameters optimization

The optimization of EWC parameters (width and height) was determined based on the TUI and throughput of the material. Since the larger EWC width resulted in better RF heating uniformity, the optimized EWC width should be as large as possible under the limit of container size and treatment throughput. Based on the results of this study, the heating uniformity TUI should not be larger than 0.3, thus, the ratio between EWC width w (m) and container length L (m) should be:

$$K_w \geq \frac{w}{L} = \frac{0.035}{0.184} \approx 0.19 \tag{10}$$

The optimized new EWC width can be calculated with the selected container length:

$$w \approx K_w L \tag{11}$$

Based on the EWC width w and treatment throughput M (kg), the maximum sample height h_m (m) with EWC can be calculated with the volume V (m^3) and density ρ (kg m^{-3}):

$$h_m = \frac{V}{S_m} \tag{12}$$

$$V = \frac{M}{\rho} \tag{13}$$

$$S_m = (W - w)(L - w) \tag{14}$$

where S_m is the bottom area of the sample (m^2), W and L are container width (m) and length (m), respectively.

The ratio between the optimum EWC height h (m) and maximum sample height h_m (m) was K_H, and data of 3 different EWC widths (15, 25 and 35 mm) in this study were used to evaluate the range of K_H values, which were listed below:

$$K_{H15} \geq \frac{h_{15}}{h_m} = \frac{0.03}{0.0416} \approx 0.72 \tag{15}$$

$$K_{H25} \geq \frac{h_{25}}{h_m} = \frac{0.04}{0.0489} \approx 0.82 \tag{16}$$

$$K_{H35} \geq \frac{h_{35}}{h_m} = \frac{0.05}{0.056} \approx 0.89 \tag{17}$$

Thus, the estimated range of K_H was 0.7–0.9 and the optimized EWC height h (m) can be calculated by:

$$h \approx K_H h_m \tag{18}$$

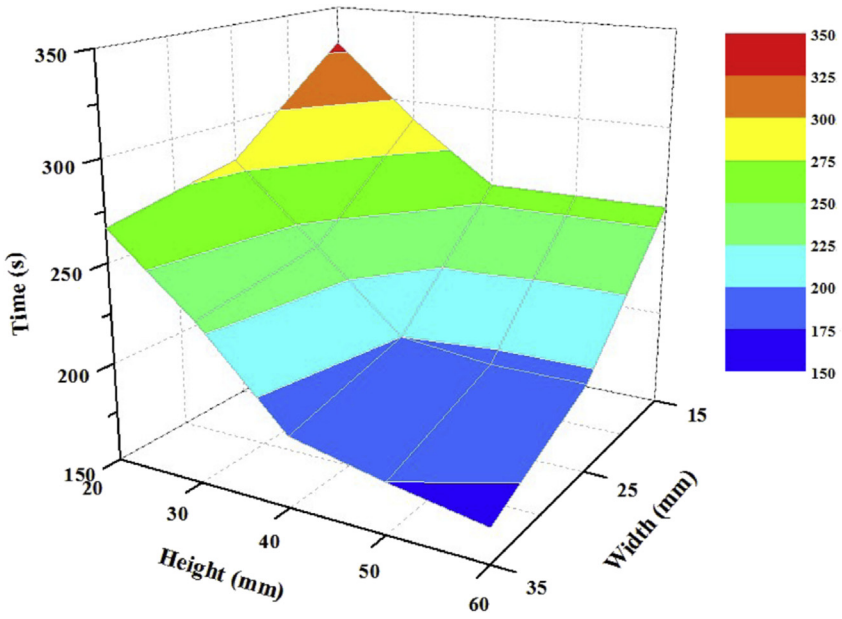

Fig. 10. RF heating times of potato starch with moisture content of 31.55% w.b. at 110 mm electrode gap to the target temperature without and with EWC sheets as a function of height and width.

Equations (10)–(18) could be used to estimate the optimized EWC parameters.

4. Conclusions

The dielectric properties and physical parameters of potato starch sample with moisture content of 31.55% w.b. were measured and determined for computer simulation. A computer model of the starch sample heated by 27.12 MHz RF electromagnetic energy was established to evaluate the heating uniformity improvement of mid-high moisture starch sample using COMSOL. The results of RF heating experiment and simulation were in good agreement based on the temperature contours comparison in top and middle layers. The introducing of EWC had clear effects to improve RF heating uniformity. As experimental and simulated results showed, the heating uniformity increased as the EWC width increased, and the best heating uniformity value at the determined EWC height would be reached before EWC exceeded its limit size. The heating rate of the sample to target temperature increased with increasing EWC size. The optimized equation was also developed to conveniently obtain the better EWC size parameters for other RF heating applications. Results of this study are potentially valuable for industrial implementations of RF energy on processing mid-high moisture materials.

Acknowledgements

This research was conducted in the Northwest A&F University and Chinese Academy of Agricultural Mechanization Sciences. This work was supported by the National Key Research and Development Plan (2016YFD0401300). The authors also thank Zhi Huang, Bo Zhang, Long Chen, Kun Wang, Bo Ling and Rui Li for their helps in conducting experiments.

References

Aviara, N.A., Onuoha, L.N., Falola, O.E., Igbeka, J.C., 2014. Energy and exergy analyses of native cassava starch drying in a tray dryer. Energy 73 (9), 809–817.
Balanis, C.A., 1989. Advanced Engineering Electromagnetics. John Wiley & Sons, New York.
Birla, S.L., Wang, S., Tang, J., Hallman, G., 2004. Improving heating uniformity of fresh fruit in radio frequency treatments for pest control. Postharvest Biol. Technol. 33 (2), 205–217.
Birla, S., Wang, S., Tang, J., 2008. Computer simulation of radio frequency heating of model fruit immersed in water. J. Food Eng. 84 (2), 270–280.
Bo, A., Tunde-Akintunde, T.Y., 2013. Effect of drying method and variety on quality of cassava starch extracts. Afr. J. Food Agric. Nutr. Dev. 13 (5), 8351–8367.
Brandrup, J., Immergut, E.H., Grulke, E.A., Abe, A., Bloch, D.R., 1989. Polymer Handbook. John Wiley & Sons, New York.
Çatal, H., İbanoğlu, Ş., 2012. Ozonation of corn and potato starch in aqueous solution: effects on the thermal, pasting and structural properties. Int. J. Food Sci. Technol. 47 (9), 1958–1963.
Chen, L., Huang, Z., Wang, K., Li, W., Wang, S., 2016. Simulation and validation of radio frequency heating with conveyor movement. J. Electromagn. Waves Appl. 30 (4), 473–491.
Choi, C.T.M., Konrad, A., 1991. Finite element modeling of the RF heating process. IEEE Trans. Magn. 27 (5), 4227–4230.
COMSOL, 2012. Material Library V4.3a. COMSOL Multiphysics, Burlington.
Farag, K.W., Marra, F., Lyng, J.G., Morgan, D.J., Cronin, D.A., 2010. Temperature changes and power consumption during radio frequency tempering of beef lean/fat formulations. Food Bioprocess Technol. 3 (5), 732–740.
Gowda, D.J., Shivaprasad, V., Ramaiah, H., 1991. Drying and storage studies on groundnut (DH-3-30) seeds (Arachis hypogeal L.). Karnataka J. agric.sci. 4 (1&2), 32–35.
Guo, W., Wang, S., Tiwari, G., Johnson, J.A., Tang, J., 2010. Temperature and moisture dependent dielectric properties of legume flour associated with dielectric heating. LWT-Food Sci. Technol. 43 (2), 193–201.
Huang, Z., Zhu, H., Yan, R., Wang, S., 2015. Simulation and prediction of radio frequency heating in dry soybeans. Biosyst. Eng. 129, 34–47.
Huang, Z., Zhang, B., Marra, F., Wang, S., 2016. Computational modelling of the impact of polystyrene containers on radio frequency heating uniformity improvement for dried soybeans. Innov. Food Sci. Emerg. Technol. 33, 365–380.
Jiao, Y., Tang, J., Wang, S., 2014. A new strategy to improve heating uniformity of low moisture foods in radio frequency treatment for pathogen control. J. Food Eng. 141, 128–138.
Jiao, Y., Shi, H., Tang, J., Li, F., Wang, S., 2015. Improvement of radio frequency (RF) heating uniformity on low moisture foods with Polyetherimide (PEI) blocks. Food Res. Int. 74, 106–114.
Juran, R., 1991. Modern Plastics Encyclopedia. McGraw-Hill, New York.
Koral, T., 2004. Radio frequency heating and post-baking. Biscuit World 7 (4), 1–7.
Ling, B., Guo, W., Hou, L., Li, R., Wang, S., 2014. Dielectric properties of pistachio kernels as influenced by frequency, temperature, moisture and salt content. Food Bioprocess Technol. 8 (2), 420–430.
Liu, Y., Tang, J., Mao, Z., Mah, J.-H., Jiao, S., Wang, S., 2011. Quality and mold control of enriched white bread by combined radio frequency and hot air treatment. J. Food Eng. 104 (4), 492–498.
Lu, X., 2015. Strategy of potato as staple food:significance, bottlenecks and policy suggestions. J. Huazhong Agric. Univ. Soc. Sci. Ed. 2015 (3), 1–7.
Ndife, M., Şumnu, G., Bayindirli, L., 1998. Dielectric properties of six different species

of starch at 2450 MHz. Food Res. Int. 31 (1), 43–52.
Nelson, S.O., 1996. Review and assessment of radio-frequency and microwave energy for stored-grain insect control. Trans. ASAE 39 (4), 1475–1484.
Noel, T.R., Ring, S.G., 1992. A study of the heat capacity of starch/water mixtures. Carbohydr. Res. 227, 203–213.
Ruan, H., Chen, Q., Fu, M., Xu, Q., He, G., 2009. Preparation and properties of octenyl succinic anhydride modified potato starch. Food Chem. 114 (1), 81–86.
Ryynänen, S., 1995. The electromagnetic properties of food materials: a review of the basic principles. J. Food Eng. 26 (4), 409–429.
SAC, 1985. Inspection of Grain and Oilseeds Methods for Determination of Moisture Content GB5497-85. Standardization Administration of the P.R. China, Beijing, China.
Sajilata, M.G., Singhal, R.S., Kulkarni, P.R., 2006. Resistant starch–a review. Compr. Rev. Food. Sci. Food Saf. 5 (1), 1–17.
Strayfield, 2012. RF Drying System Model SO6B User Manual. Strayfield International, Wokingham, UK.
Talburt, W.F., Smith, O., 1987. Potato Processing, fourth ed. Van Nostrand Reinhold, New York, pp. 647–663.
TEC, 1987. Radio Frequency Dielectric Heating in Industry. Thermo Energy Corporation, Palo Alto, California, pp. c1–c6.
Tiwari, G., Wang, S., Tang, J., Birla, S., 2011. Analysis of radio frequency (RF) power distribution in dry food materials. J. Food Eng. 104 (4), 548–556.
Von Hippel, A., 1954. Dielectric Properties and Waves. John Wiley & Sons, New York.
Wang, S., Tang, J., 2001. Radio frequency and microwave alternative treatments for insect control in nuts: a review. Agric. Eng. J. 10 (3&4), 105–120.
Wang, S., Tiwari, G., Jiao, S., Johnson, J.A., Tang, J., 2010. Developing postharvest disinfestation treatments for legumes using radio frequency energy. Biosyst. Eng. 105 (3), 341–349.
Wang, Y., Li, Y., Wang, S., Zhang, L., Gao, M., Tang, J., 2011. Review of dielectric drying of foods and agricultural products. Int. J. Agric. Biol. Eng. 4 (1), 1–19.
Wang, K., Chen, L., Li, W., Wang, S., 2015a. Evaluating the top electrode voltage distribution uniformity in radio frequency systems. J. Electromagn. Waves Appl. 29 (6), 1–11.
Wang, K., Zhu, H., Chen, L., Li, W., Wang, S., 2015b. Validation of top electrode voltage in free-running oscillator radio frequency systems with different moisture content soybeans. Biosyst. Eng. 131, 41–48.
Zavareze, E.D.R., Storck, C.R., Castro, L.A.S.D., Schirmer, M.A., Dias, A.R.G., 2010. Effect of heat-moisture treatment on rice starch of varying amylose content. Food Chem. 121 (2), 358–365.
Zhang, S., Zhou, L., Ling, B., Wang, S., 2016. Dielectric properties of peanut kernels associated with microwave and radio frequency drying. Biosyst. Eng. 145, 108–117.
Zhu, H., Huang, Z., Wang, S., 2014. Experimental and simulated top electrode voltage in free-running oscillator radio frequency systems. J. Electromagn. Waves Appl. 28 (5), 606–617.